euspen's 20th International Conference & Exhibition, Geneva, CH, June 2020
www.euspen.eu

# A compact and calibratable von Hamos X-Ray Spectrometer based on two full-cylinder HAPG mosaic crystals for high energy-resolution XES and RIXS

Ina Holfelder[1], Rolf Fliegauf[1], Yves Kayser[1], Matthias Müller[1], Malte Wansleben[2], Jan Weser[1], Burkhard Beckhoff[1]

[1] *Physikalisch-Technische Bundesanstalt, Abbestr. 2-12, 10587 Berlin*
[2] *Helmholtz Zentrum Berlin für Materialien und Energie, Department of Optics and Beamlines, Albert-Einstein-Str. 15,12489 Berlin, Germany*

*Ina.holfelder@ptb.de*

**Abstract**
In high-resolution X-ray Emission Spectroscopy (XES) crystal-based Wavelength-Dispersive Spectrometers (WDS) are applied to examine the elemental and chemical speciation of different compounds. Thereby, the so-called von Hamos geometry provides improved detection efficiency when compared to flat crystal configurations due to sagittal focusing using cylindrically bent crystals. To maximize the detection efficiency, a full-cylinder optic equipped with a mosaic crystal can be applied.
A novel calibratable von Hamos X-ray spectrometer based on one to two full-cylinder optics was developed at the PTB. To realize the full-cylinder geometry, Highly Annealed Pyrolytic Graphite (HAPG) was used. Not only does this mosaic crystal possess good bending properties, but it also shows highly integrated reflectivity while offering low mosaicity - ensuring high resolving power. The spectrometer enables measurements on X-ray emission lines and radiation in an energy range from 2.4 keV (0.52 nm) up to 18 keV (0.07 nm). Using synchrotron radiation as a tunable excitation source, resonant inelastic X-ray scattering (RIXS) can be carried out with the spectrometer. The spectrometer combines high detection efficiency with medium to high energy resolution in a compact arrangement. This aspect makes the instrument suitable for laboratory arrangements. The design and commissioning of the spectrometer are presented in this article. Also, a concept for the automated alignment procedure is discussed.

Analysis, Automation, Calibration, Image, Measuring Instrument, Metrology, X-ray

## 1. Introduction

The demand for new nano energy and composite materials is growing rapidly in high performance applications such as for automotive or aerospace engineering. In order to link the material properties and performances to their physical and chemical composition, detailed non-destructive analysis is necessary. Reference-free X-ray fluorescence analysis enables the probing of the composition without the need for reference materials. These materials are often only available at a limited scale, since they need to be representative enough of the specimen under investigation [1, 2]. Hence, there is a need for reference-free methods, which refer to methods that are independent from any reference or calibration sample. Aside from using X-ray emission spectroscopy, chemical speciation can be realized by means of X-ray emission spectroscopy (XES) or resonant inelastic X-ray scattering (RIXS) [3, 4, 5]. The latter method can only be performed with a tunable monochromatic X-ray source, such as synchrotron radiation, which can cause radiation damage on the sample. To prevent this, new efficient detection systems are needed.

For this purpose, a new wavelength-despersive spectrometer (WDS) was developed and taken into operation at the Physikalisch-Technische Bundesanstalt (PTB). To ensure efficient and reference-free XES or RIXS analysis, the following specifications must be met. The spectrometer should enable high- resolving and efficient detection for measurements on the chemical species of 3d transition metals, for example. For reference-free analysis, calibratable instrumentation is required. From a mechanical point of view, this can be realized through a rigid construction of the spectrometer as well as by a high reproducibility and accuracy of the positioning system for all optical components. A further requirement was the compactness and flexibility of the spectrometer.

The following describes how the requirements of the spectrometer design were met. The characterization of the spectrometer is also discussed and a concept of an automated alignment procedure is introduced.

## 2. Spectrometer design

To realize a spectrometer with high energy resolution and high detection efficiency, full-cylinder optics in the von Hamos geometry [6, 7], where incident X-ray radiation is dispersed by Braggs law, were used, (see Figure 1). For the position-resolved detection of the Bragg-reflected X-ray radiation, an X-ray charge coupled device (CCD) camera is used. The dispersive element used for the optics is the highly-flexible crystal *Highly Annealed Pyrolytic Graphite (HAPG)*, which is fixed by adhesion onto a Zerodur® substrate with a 100 mm inner diameter.

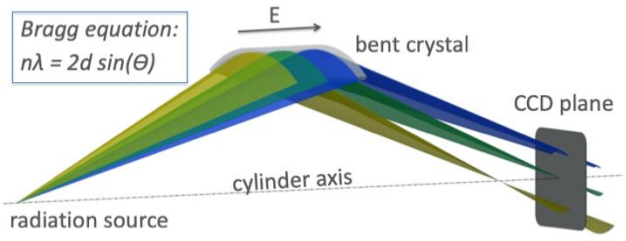


**Figure 1.** Principle of the von Hamos geometry

In Figure 2, the frontal part of the spectrometer, which can be fixed at an experimental chamber with a DN 150CF flange or

larger size, is shown. The spectrometer can integrate three optics, whereby just two are used at the moment. To align the optics, a 5-axis piezo manipulator is installed for each optic. A detailed description of the piezo stages is given in [8]. Additionally, the CCD camera can be aligned by three linear piezo stages. In the von Hamos geometry, the distances between the X-ray radiation source and the optic, as well as between the optic and the CCD detector, depend on the Bragg equation and increase for higher photon energies (shallower Bragg angles). The positioning system for the optical components allows for the detection of photon energies from 2.4 kev (λ=0.52 nm) to 18 keV (λ=0.07 nm) in the first order of reflection, which correspond to the Bragg angles of 50.4° to 5.9°. For energies above 10 keV (λ=0.12 nm), a reduced reflectivity of the crystals and detection efficiency of the CCD camera must be adjusted for.

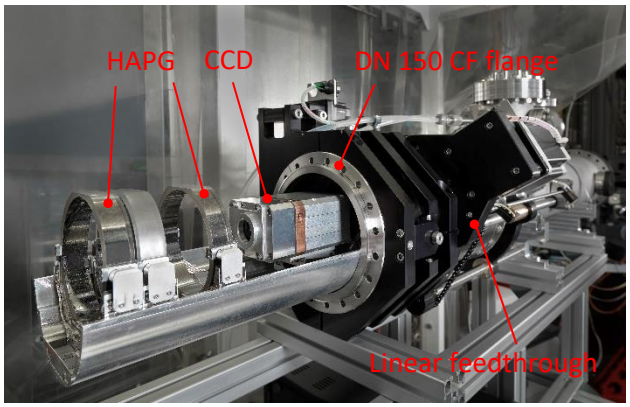


**Figure 2.** Front view of the von Hamos spectrometer

For radiometrical calibration in each detection position on the energy axis, the detection efficiency as well as the spectrometer response must be known. Therefore, a precise positioning and alignment of the optics is necessary. To reduce the calibration effort, a rigid construction of the rail bed is necessary. Further information regarding the calibration can be found in [9]. Since the rail bed is cantilever-fixed onto the experimental chamber flange, some deformation of the structure must be expected. Therefore, finite element simulations were performed to create the optimal rail bed shape with reduced deformation. To enable high reproducibility and accuracy, all optical components move on the same 1200 mm long linear guide. The units holding the optical elements and the CCD camera can be positioned independently from one another, which enables three different operation modes. In the first operating mode, the optics used on the monitored energy range: the first one in the energy range from 2.4 keV (λ=0.52 nm) to 10 keV (λ=0.12 nm) and the second one for the higher energy range, up to 18 keV (λ=0.07 nm). In the second operating mode, the emission lines can be measured in the second reflection order of the crystal. A significant increase of resolution could be achieved, but this is accompanied by a loss of intensity. The use of two optics for the double Bragg reflection represents the last mode of operation. Again, the resolution could be increased. At the same time, however, the intensity of the detected signal is further reduced.

To guarantee an optimal performance in each operation mode, the spectrometer was characterized after assembly.

## 3. Characterization of the spectrometer

The characterization of the spectrometer can be divided into two parts: the characterization of the dispersive optics and the characterization of the linear guide.

Before the optics could be designed, comprehensive studies of the diffraction properties of the HAPG as well as the proper substrate materials were performed, which are described in detail in [10]. Since the shape of the cylinder-substrate affects the resolution of the detected spectrum, the optics are inspected for flatness and roundness with a form gauge before coating them with the HAPG film. The roughness of the inside surface of the cylinder is measured. After coating, the reflection properties of the optics are analyzed with synchrotron radiation.

Subsequently, the linear guide system is examined along the entire travel path with an autocollimator for angular error and straightness. The individual piezo motor axes are also examined.

### *3.1. Characterization of the optics*

To investigate the diffraction properties of the HAPG optics, so-called rocking curves are measured in a separate experiment at different positions on the optics inner surface. To detect the rocking curve, the angle of incidence is varied in the vicinity of the energy-dependent Bragg angle and in each step the signal reflected by the HAPG crystal is detected by a photo diode.

In Figure 3, the peak reflectivities along the cylinder axis, determined from the rocking curves and averaged from several measurement points over the entire height of the optical cylinder in 0.5 mm increments, are shown. The measurements were carried out at the BAMline (BESSY II) using monochromated synchrotron radiation of 8.046 keV (λ=0.154 nm) with a beam size of 1.5 mm x 2.8 mm. Based on this scan, the inhomogeneity of the cylinder is clearly visible. The maximum peak reflectivity of about 36 % can be found at motor position at -1.5 mm from the center of the cylinder height. To the right of the center, a drop by about 10 % towards a minimum in the the peak reflectivity is observed. At both edges of the optics, the peak reflectivity decreases significantly until it drops to zero in the left margin, indicating that the adhesion of the HAPG layers to the edges decreases.

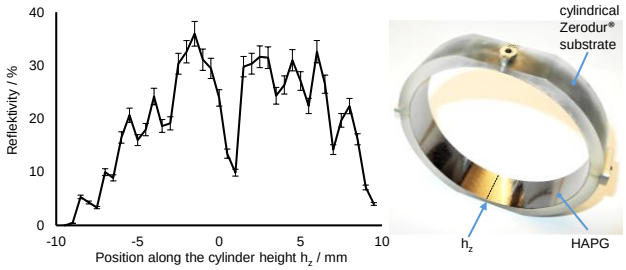


**Figure 3.** Peak reflectivities along cylinder height in 0.5 mm increments

Large deviations from the desired shape lead to spectral broadening. Therefore, measurements were performed with a form tester MMQ 400 from Mahr GmbH, Goettingen. The measured value is recorded in 0.02 ° step increments. The concentricity of the inner surface of the cylinder is measured at five positions, at the positions -10 mm, -5 mm, 0 mm, +5 mm, +10 mm from the center. At the end, the total concentricity is determined. The radial concentricity tolerance is 5 µm to the axis of symmetry and the perpendicularity is 2 µm between the axis of symmetry and the side surface of the cylinder. To ensure good adhesion of the HAPG layer, the surface finish of the substrates must match the surface quality of optical material. Therefore, an arithmetic mean roughness value Ra of 4 nm for the optical surface is required. This is achieved in a polishing process that follows machining.

Furthermore, the surface quality of HAPG was tested with a light microscope and the layer thickness was estimated by means of a profilometer relative to the substrate surface.

In summary, the tests show that the HAPG material is inhomogeneous with regard to its optical properties, which in turn are dependent on the substrate quality. Nevertheless, HAPG crystals have several advantages over other mosaic crystals or ideal crystals. They combine a high integral reflectivity with a high resolution capability. The layers can be easily bent to a radius as small as 50 mm without showing any degradation. The advantages in this application clearly outweigh the disadvantage of lateral inhomogeneity. A spectral resolution of $E/\Delta E > 2700$ could be measured with the presented spectrometer using two optics [12].

### *3.2. Characterization of the linear guide*

In order to keep the adjustment effort as low as possible, the deflection of the rail bed and the movement behaviour of the linear guide system was validated. In Figure 4 the rail bed in the frontal view is shown. Due to the cantilevered mount on the experimental chamber flange, manufacturing or assembly-related errors, straightness, and angular deviations of the guide rail are expected. All errors can cause a rotation of the crystals, so that the Bragg equation is not met properly. To estimate the system behaviour, the motion behaviour of the entire system was characterized.

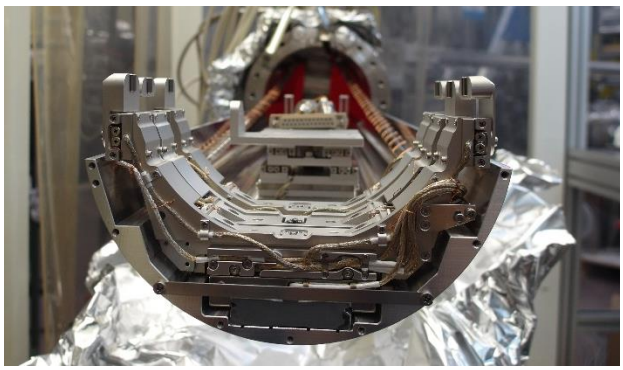

**Figure 4.** Linear rail bed including the linear guide system and the piezo stages in a frontal view

The motion behaviour of the individual axes of the multi-axis piezo positioning system is surveyed with an autocollimator. With an autocollimator both relevant motion errors (yaw and pitch error) can be detected. To ensure the reproducibility of the linear movement, several measuring cycles were repeated. According to X-ray diffraction experiments, the deviation of the yaw and pitch error should be less than ±0.04°.
In Figure 5, pitch behaviour along the 1200 mm long linear guide is shown as an example.

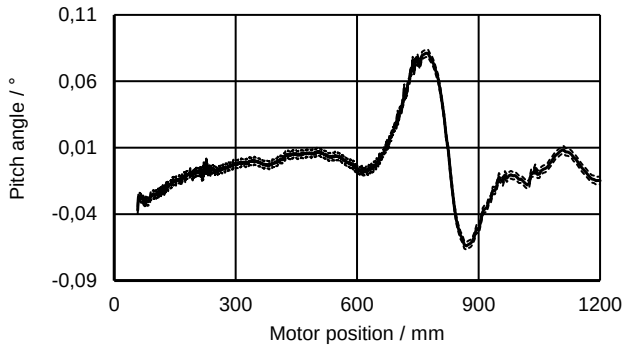


**Figure 5.** Pitch error of the 1200 mm long linear guide system

A local minimum is observed in pitch behaviour at a motor position of about 620 mm, which then rises steeply, until reaching a maximum at about 780 mm. Thereafter, the course of the pitch behaviour drops back to a minimum at 870 mm. One possible reason for this is that the rail, on which all three carriages run, is not bolted to the rail bed at the location of the spectrometer flange in which the rail bed is suspended. This was not possible by design and may cause the rail to deform in this area, thereby affecting the straightness of the carriage movement. Also, uneven tightening of the screws (which are not unifom from the rail start or the middle of the rail) can cause tension on the rail.

The great variation in the motion errors between 600 mm and 900 mm cause a deviation of the optic from its optimal position. Therefore, an improvement of the linear guide system or a realignment of the optical components at different positions is necessary. Based on the given assembly space, a reinforcement of the linear guide system was not possible. Due to the transportability of the spectrometer and the second translational degree of freedom (linear feedthrough) which runs parallel to the linear guide, too many unknown parameters are introduced. Thus, a compensation based on the characterization was also not possible and instead a first concept of an alignment procedure was developed.

## 4. Alignment procedure

Within the scope of this work, a concept for an automated adjustment procedure for alignment of the optical components, both HAPG optics and the CCD camera, has been developed. The focus was on ensuring that the procedure is as fast and reliable as possible. Therefore, the circular Bragg-reflected signal detected by CCD is analyzed.

The steps necessary for the development and use of the procedure are described below, where the concept of the automated alignment procedure is explained in greater detail. The algorithms to evaluate the criteria have been programmed using the Interactive Data Language (IDL), as it is especially suitable for the analysis and visualization of data.

### *4.1. Raytracing simulations for the resolution analysis*

To develop an image evaluation procedure, possible deviations from the ideal optic position were simulated in advance with a ray-tracing algorithm. Here, a Monte Carlo ray-tracing algorithm, based on the work of Beckhoff [13] and extended by Anklamm [14], was used. From the results of the ray-tracing simulations the change of the circular Bragg signal and thereby the degradation of the spectral resolution could be validated depending on the deviation from the ideal optic position.

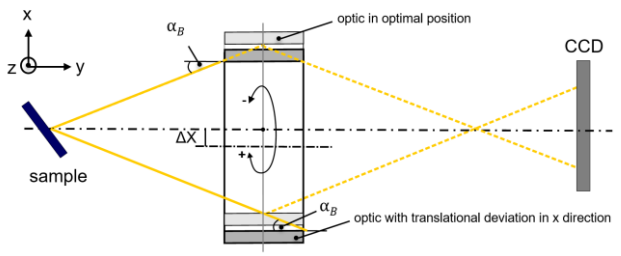


**Figure 6.** Schematic top-down view of the beam path using one optic for Bragg reflection

On the one hand, the translational deviations in the x- and z-direction were examined, as well as the rotatory deviations around the z- and x-axis, figure 6. At a distance of 9 mm behind the image focus plane of the copper $K\alpha_1$ line, the copper $K\alpha_{1,2}$ lines were simulated. In order to be able to better assess the effect of the crystal misalignment and the change in the spectrum, the two spectral lines $K\alpha_1$ and $K\alpha_2$ have been simulated with equal transition probabilities. The number of simulated photons

incidenting to the crystal is 10 million and these simulated photons may be detected by the CCD camera. Simulated copper $K\alpha_{1,2}$ lines with rotational deviations from optimal position (left) and without deviation (right) are shown in Figure 7.

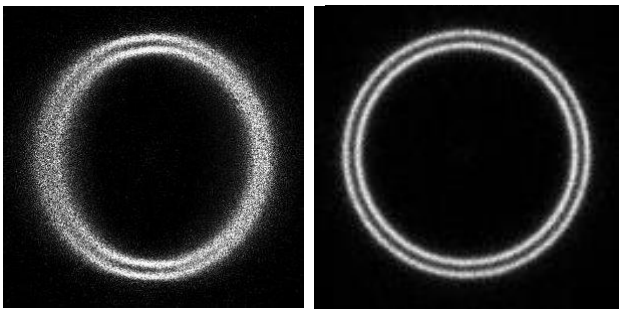

**Figure 7.** Simulated Cu $K\alpha_{1,2}$ lines with rotational deviations from optimal position (left) and without deviation (right)

To assess the change in the detected Bragg reflection as a function of the optic shift with respect to the source, the CCD image must be transformed into a X-ray emission spectrum. The CCD image is split from the center into radial channels. Each radial channel is defined by the distance from the center and each pixel equidistant from the center is assigned to the corresponding channel. Subsequently, all pixels of a radial channel are integrated.

To analyze the spectral resolution degradation due to misalignment, translational and rotational displacements are simulated and compared to the simulated spectra with no displacement with respect to the ideal position. On the basis of the simulations, suitable criteria for the image evaluation are determined.

### *4.2. Alignment procedure*

The alignment procedure is divided into different sections and consists of a main program and two subroutines. The main program forms the framework for image processing. It stores the current motor positions and queries the user about all relevant parameters, such as energy of the spectral lines to be detected, number of dispersive elements used, etc. Based on these transferred start values, all components are moved to their target positions. Then the first subroutine for image acquisition is called and the adjustment of the HAPG optics starts, whereby both optics have to be adjusted individually one after the other at their respective positions. At the beginning, the two translational axes of the HAPG optics are adjusted. A subroutine traverses a defined scan area around the current value of the respective motor in a specified step size and triggers the CCD camera, which takes a picture after each motor step. After each motor scan, the second subroutine is started. This subroutine is an image evaluation procedure that includes the three steps of image processing, image analysis and image evaluation. The dark image is subtracted during image processing. Various properties of the spectra, such as *spectrum intensity*, the *area between both peaks*, *full width at half maximum of both peaks*, *maximum value of the dominant peak* and *the difference of the maximum values of the integrated row or column profiles*, are determined in the image analysis. A detailed description of the different criteria is explained in [11]. These criteria are compared with one another in the image evaluation routine in order to calculate an optimal position of the optics. In the last step of the image evaluation procedure, the results can also be visualized. Once the translatory axes have been varied and evaluated, the two rotary axes of the HAPG optics are adjusted. All four motor axes are aligned iteratively. If the calculated optimal positions remain within the specified tolerance range, the loop is ended. Afterwards, the calculated positions are transferred to the motors and reconciled. When the adjustment for one dispersive element is completed, the procedure for the second optic is repeated.

Initial investigations have shown that the inhomogeneity of the real crystals may result in data misinterpretations during the alignment procedure. In the current state of the algorithm, the performed automated alignment is not satisfactory. On this point, future research aimed at implementing circular fitting procedures of the CCD data attaining robust alignment procedures is necessary.

## 5. Summary

Within the frame of this work, a new calibratable wavelength-dispersive spectrometer has been developed. Due to the von Hamos geometry the spectrometer is efficient, flexible and compact in size. Different operation modes enable the optimal exploitation of the instrument.

The characterization of the linear guide system has shown that the construction of the rail bed, which is cantilevered on a flange, does not meet all the desired requirements. This makes it necessary to realign the optics for various energy settings. An automated adjustment is advantageous and serves to speed up the process. For this purpose, a basic version of a procedure was created and described as a first successful approach to automated adjustment.

The successfully performed XES experiments with synchrotron radiation on battery electrodes [11] create the framework for technology transfer. Due to its compactness, its high efficiency and its high resolving power, the developed spectrometer represents a detection system which, when operated with a laboratory radiation source and with minimal design changes, can be transformed into a tabletop device. An optimized adjustment algorithm must be developed for commercial operation and reliable calibration. It can be expected that this class of high-resolution X-ray spectrometers can be used successfully for ex-situ, in-situ and operando investigations of energy materials.

## References


[1] Beckhoff B 2008 *J. Anal. At. Spectrom.* **23** 845
[2] Beckhoff B, Fliegauf R, Kolbe M, Müller M, Weser J and Ulm G 2007 *Anal. Chem* **79** 7873
[3] Kavcic M, Bukar K, Petric M, Zitnik M, Arcon I, Dominko R and Vizentin A 2016 *J. Phys. Chem. C* **120** (43) 24568
[4] Sa J, Kayser Y, Milne C J, Abreu Fernandes D L and Szlachetko J 2014 *Phys. Chem. Chem. Phys.* **16** 7692
[5] Bauer M 2014 *Phys. Chem. Chem. Phys.* **16** 13827
[6] Hamos L v 1932 *Naturwissenschaften* **20** 705 - 706
[7] Anklamm L, Schlesiger C, Malzer W, Grötzsch D, Neitzel M and Kanngießer B 2014 *Review of Scientific Intruments* **85** 053110-1-053110-5
[8] Holfelder I, Fliegauf R, Kayser Y, Müller M, Wansleben M, Weser J, and Beckhoff B 2018, doi: 10.18429/JACoW-MEDSI2018-WEOPMA06
[9] Wansleben M, Kayser Y, Hönicke P, Holfelder I, Wählisch A, Unterumsberger R and Beckhoff B 2019 *Metrologia* **56** 065007
[10] Gerlach M, Anklamm L, Antonov A, Grigorieva I, Holfelder I, Kanngießer B, Legall H, Malzer W, Schlesiger C and Beckhoff B 2015 *J. Appl. Cryst.* **48** 1381-1390
[11] Holfelder I 2018 PhD thesis, Technische Universität Berlin, Berlin
[12] Wansleben M, Vinson J, Holfelder I, Kayser Y and Beckhoff B 2019 *X-ray Spec.* **48** 102
[13] Beckhoff B 1995 PhD thesis, University Bremen, Bremen
[14] Anklamm L 2010, Diploma thesis, Technical University Berlin, Berlin